J|A|C|S
ARTICLES
Published on Web 04/03/2004

Assignment of the Backbone Resonances for Microcrystalline Ubiquitin

Tatyana I. Igumenova,[†,#] A. Joshua Wand,[‡] and Ann E. McDermott*[,†]

Contribution from the Department of Biochemistry and Biophysics, University of Pennsylvania, The Johnson Research Foundation, Philadelphia, Pennsylvania 19104, and Department of Chemistry, Columbia University, 3000 Broadway MC 3113, New York, New York 10027

Received September 22, 2003; Revised Manuscript Received February 4, 2004; E-mail: aem5@columbia.edu

Abstract: Site-specific assignments for the solid-state NMR spectra of uniformly ^{13}C,^{15}N-enriched ubiquitin are described. The assignments are derived from three three-dimensional $^{15}N-^{13}C-^{13}C$ correlation spectra collected at 400 MHz on microcrystalline material. A few residues (the loop near Threonine 9 and the C-terminal fragment) were missing and correspond to regions previously reported to be mobile on the basis of X-ray crystallography and solution NMR studies. A few additional sites exhibit shifts that differ from previously reported solution NMR assignments. Nonetheless, these de novo assignments indicate close agreement between the chemical shifts observed in solution and those in microcrystalline or precipitated solids. The methods utilized are likely to be generally applicable for other noncrystalline, nonsoluble proteins.

Introduction

While significant progress has been made in all aspects of protein structure determination by solid-state NMR, site-specific assignments of uniformly labeled proteins remain an important checkpoint in any de novo structure. We describe here a direct and robust protocol for assignments, reporting its successful implementation on a test system, ubiquitin. Human ubiquitin is an opportune protein for illustrating an assignment protocol since it is relatively small (76 residues, 8.6 kDa), thermally stable, and has mixed secondary structure. Extensive literature about its solution NMR properties is available,[1−6] and the X-ray diffraction coordinates are known as well.[7] We have used this system to illustrate that high quality spectra at moderate and high magnetic fields are readily attained and to explore the principal issues that limit the resolution in solid-state NMR of uniformly enriched materials. One of the first examples of successful assignment efforts was the study of uniformly ^{13}C,^{15}N-enriched ubiquitin (76 residues, 8.6 kDa) carried out by Straus et al.[8] using two-dimensional (2D) $^{13}C/^{15}N$ chemical shift correlation spectroscopy. The assignment of lyophilized ubiquitin was also reported by Hong;[9] the experimental strategy included a combination of 2D and 3D NMR methods and implementation of a novel isotope labeling scheme.[10] Both studies yielded partial (∼25%) site-specific assignments of ubiquitin, with further assignment efforts impeded by low spectral resolution due to usage of moderate applied magnetic field strengths (7.0−9.4 T) and lyophilized or rehydrated protein samples.

It became evident early on that a key to the success of assignments efforts in solid-state NMR is the sample preparation protocols and their profound effects on the line widths. NMR lines of freeze-dried proteins and peptides are usually inhomogeneously broadened. Hydration of freeze-dried samples was shown to improve the spectral resolution in ^{13}C CP MAS spectra of natural abundance lysozyme[11] and ubiquitin.[12] In the latter case, $^{13}CH_2$ line widths of >2 ppm and ∼1.3 ppm were reported for uniformly and "selectively and extensively" ^{13}C-enriched samples, respectively. Addition of cryoprotectants such as trehalose and poly(ethylene glycol) improved ^{31}P line widths in a lyophilized ternary complex of a 46 kDa enzyme with its substrate and inhibitor.[13] Many globular proteins, when prepared as solids through controlled precipitation or crystallization, have been shown to give narrow NMR lines: staphylococcal nuclease,[14] α-lytic protease,[15] BPTI,[16] SH3 domain of α-spectrin,[17]

† Columbia University.
‡ University of Pennsylvania.
# Present address: Department of Biochemistry and Biophysics, University of Pennsylvania, Philadelphia, PA 19104.

(1) DiStefano, D. L.; Wand, A. J. *Biochemistry* **1987**, *26*, 7272−7281.
(2) Weber, P. L.; Brown, S. C.; Mueller, L. *Biochemistry* **1987**, *26*, 7282−7290.
(3) Wand, A. J.; Urbauer, J. L.; McEvoy, R. P.; Bieber, R. J. *Biochemistry* **1996**, *35*, 6116−6125.
(4) Tjandra, N.; Feller, S. E.; Pastor, R. W.; Bax, A. *J. Am. Chem. Soc.* **1995**, *117*, 12562−12566.
(5) Cornilescu, G.; Marquardt, J. L.; Ottiger, M.; Bax, A. *J. Am. Chem. Soc.* **1998**, *120*, 6836−6837.
(6) Babu, C. R.; Flynn, P. F.; Wand, A. J. *J. Am. Chem. Soc.* **2001**, *123*, 2691−2692.
(7) Vijaykumar, S.; Bugg, C. E.; Cook, W. J. *J. Mol. Biol.* **1987**, *194*, 531−544.
(8) Straus, S. K.; Bremi, T.; Ernst, R. R. *J. Biomol. NMR* **1998**, *12*, 39−50.
(9) Hong, M. *J. Biomol. NMR* **1999**, *15*, 1−14.
(10) Hong, M.; Jakes, K. *J. Biomol. NMR* **1999**, *14*, 71−74.
(11) Gregory, R. B.; Gangoda, M.; Gilpin, R. K.; Su, W. *Biopolymers* **1993**, *33*, 513−519.
(12) Hong, M. *J. Magn. Reson.* **1999**, *139*, 389−401.
(13) Jakeman, D. L.; Mitchell, D. J.; Shuttleworth, W. A.; Evans, J. N. S. *J. Biomol. NMR* **1998**, *12*, 417−421.
(14) Cole, H. B. R.; Torchia, D. A. *Chem. Phys.* **1991**, *158*, 271−281.
(15) Smith, S. O.; Farrjones, S.; Griffin, R. G.; Bachovchin, W. W. *Science* **1989**, *244*, 961−964.
(16) McDermott, A.; Polenova, T.; Bockmann, A.; Zilm, K. W.; Paulsen, E. K.; Martin, R. W.; Montelione, G. T. *J. Biomol. NMR* **2000**, *16*, 209−219.

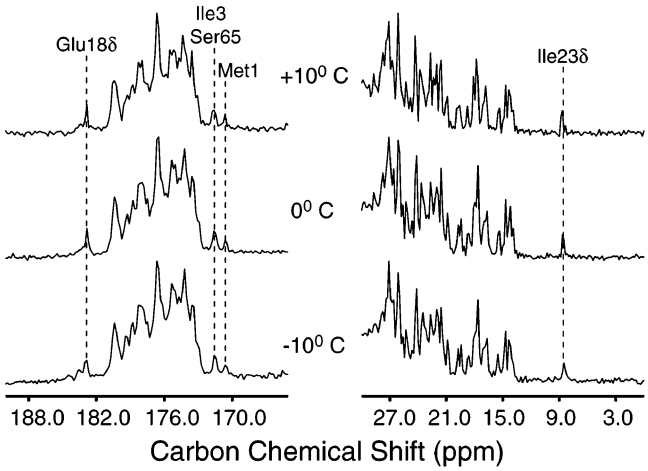

Figure 1. Expansions of ^{13}C CP MAS spectra of natural abundance ubiquitin, showing the carbonyl region (left column) and the aliphatic region (right column), collected at −10, 0, and +10 °C. Each spectrum represents 12.8 h of acquisition.

ubiquitin,[18] and triose phosphate isomerase.[19] Consequently, more progress for site-specific assignments has been made with microcrystalline samples of soluble proteins. BPTI (57 residues, 6.5 kDa)[16] was partially assigned at 800 MHz. The SH3 domain of α-spectrin (62 residues, 7.2 kDa) has been the first protein for which almost complete de novo assignments were reported.[20,21] In this work, we present site-specific backbone assignments for microcrystalline ubiquitin, obtained by somewhat different pulse sequences than that for the SH3 domain.

Materials and Methods

Uniformly ^{13}C,^{15}N-enriched ubiquitin was prepared as described previously.[3] The level of isotope enrichment was >99% for both nuclei. About 15 mg of uniformly ^{13}C,^{15}N-enriched ubiquitin was crystallized by a batch method in 60% 2-methyl-2,4-pentanediol (MPD), 20 mM citrate buffer, pH 4.0−4.2. The microcrystalline precipitate was centrifuged for 20 min at 9000 rpm and transferred to the NMR rotor. Silicon rubber disk inserts were used to prevent sample dehydration in the course of NMR experiments.

Three-dimensional ^{13}C/^{15}N chemical shift correlation solid-state NMR spectra were acquired on a Varian/Chemagnetics Infinity Plus 400 spectrometer operating at Larmor frequencies of 396.8 MHz for ^{1}H, 99.8 MHz for ^{13}C, and 40.2 MHz for ^{15}N, using a 4-mm triple resonance T3 MAS probe (Varian Instruments), with a spinning frequency of 9 kHz and a sample temperature of 0 °C. The effect of temperature on the quality of the ^{13}C CP MAS spectra of ubiquitin was investigated in a rather limited temperature range, from −10 °C to +10 °C, using a natural abundance protein sample. Figure 1 shows expansions of the carbonyl and aliphatic regions of the ^{13}C CP MAS spectra of natural abundance ubiquitin. The given temperature values correspond to the reading of a thermocouple positioned at the end of the variable temperature gas flow line; the true temperature of the sample is higher than the thermocouple reading due to heating induced by magic angle spinning (5−10 °C). In this temperature range, very minor changes occur in the carbon spectra, as we have ascertained.

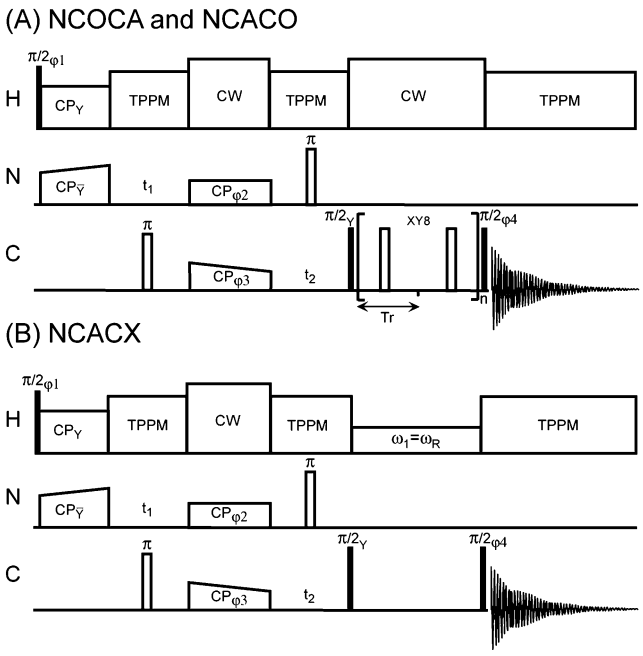

Figure 2. 3D pulse sequences used in the experiments for sequential backbone assignment. (A) NCOCA and NCACO. (B) NCACX. The following phase-cycling scheme was used: $\varphi 1 = (x\bar{x})_8$, $\varphi 2 = (\bar{y}\bar{y}yy)_4$, $\varphi 3 = (xx\bar{x}\bar{x})_4$, $\varphi 4 = (y)_4(\bar{x})_4(\bar{y})_4(x)_4$, and $\varphi_{REC} = (x\bar{x})_2(y\bar{y})_2(\bar{x}x)_2(\bar{y}y)_2$. ^{15}N−^{13}C J-decoupling was carried out with π pulses applied on the ^{15}N channel and ^{13}C channels during the corresponding evolution periods.

Three 3D experiments were carried out: (i) NCOCA experiment for interresidue backbone correlations, (ii) NCACO experiment for intraresidue backbone correlations, and (iii) NCACX experiment for backbone−side chain correlations. A cartoon of the pulse sequence used to collect NCOCA and NCACO data sets is shown in Figure 2A. ^{1}H−^{15}N cross-polarization was carried out using a ramped radio frequency field on the ^{15}N channel,[22] with the field strengths of $\omega_1(^1H) = 59$ kHz and $\omega_1(^{15}N) = 50$ kHz (ramp center), ramp size of 7.8 kHz, and a contact time of 3 ms. The double cross-polarization sequence[23] (DCP), implemented selectively,[24] was used to direct the polarization transfer from nitrogen atoms to carbonyls in a NCOCA experiment or to Cα carbons in a NCACO experiment. The duration of the cross-polarization step was 6 ms, with $\omega_1(^{15}N) = 22.5$ kHz, $\omega_1(^{13}C) = 13.5$ kHz (ramp center), and ramp size of 2.1−2.6 kHz. Homonuclear ^{13}C−^{13}C mixing was accomplished using radio frequency driven dipolar recoupling (RFDR) sequence[25] with a mixing time of 1.33 ms. π pulse duration was 7.4 μs, and the pulses were phase-cycled according to the XY-8 scheme.[26] Care was taken to mismatch ^{13}C and ^{1}H field strengths during mixing.[27] A pulse sequence for the NCACX experiment is shown in Figure 2B. ^{13}C−^{13}C spin diffusion assisted by ^{1}H irradiation, i.e., "^{13}C−^{1}H dipolar-assisted rotational resonance" experiment [28] was used to transfer polarization from Cα to Cβ, with a mixing time of 6.7 ms. Although this mixing time was optimized to mainly obtain one-bond CαCβ correlations, we also observed a number of two-bond transfers in our spectra.

(17) Pauli, J.; van Rossum, B.; Forster, H.; de Groot, H. J. M.; Oschkinat, H. *J. Magn. Reson.* **2000**, *143*, 411−416.
(18) Igumenova, T. I.; Martin, R.; Rienstra, C. M.; Paulson, E.; Wand, A. J.; Zilm, K. W.; McDermott, A. E. Presented at the Experimental NMR Conference, Orlando, FL, 2001; Poster 107.
(19) McDermott, A. Presented at the XXth International Conference on Magnetic Resonance in Biological Systems, Toronto, Canada, 2002.
(20) Pauli, J.; Baldus, M.; van Rossum, B.; de Groot, H.; Oschkinat, H. *ChemBioChem* **2001**, *2*, 272−281.
(21) van Rossum, B. J.; Castellani, F.; Rehbein, K.; Pauli, J.; Oschkinat, H. *ChemBioChem* **2001**, *2*, 906−914.
(22) Metz, G.; Wu, X. L.; Smith, S. O. *J. Magn. Reson., Ser. A* **1994**, *110*, 219−227.
(23) Schaefer, J.; McKay, R. A.; Stejskal, E. O. *J. Magn. Reson.* **1979**, *34*, 443−447.
(24) Baldus, M.; Petkova, A. T.; Herzfeld, J.; Griffin, R. G. *Mol. Phys.* **1998**, *95*, 1197−1207.
(25) Bennett, A. E.; Rienstra, C. M.; Auger, M.; Lakshmi, K. V.; Griffin, R. G. *J. Chem. Phys.* **1995**, *103*, 6951−6958.
(26) Gullion, T.; Baker, D. B.; Conradi, M. S. *J. Magn. Reson.* **1990**, *89*, 479−484.
(27) Bennett, A. E.; Rienstra, C. M.; Griffiths, J. M.; Zhen, W. G.; Lansbury, P. T.; Griffin, R. G. *J. Chem. Phys.* **1998**, *108*, 9463−9479.
(28) Takegoshi, K.; Nakamura, S.; Terao, T. *Chem. Phys. Lett.* **2001**, *344*, 631−637.

The phase cycle for all 3D experiments consisted of 16 steps and included (i) ^{1}H spin temperature alternation (two steps), (ii) suppression of the direct ^{1}H−^{13}C transfer during DCP mixing by simultaneous alternation of ^{15}N and ^{13}C spin-lock phases (two steps), and (iii) a selection of the $\pm 1 \rightarrow -1$ coherence pathway (four steps).[29] This phase cycle was sufficient to produce artifact-free 3D spectra. The number of scans per time increment was 16, and the recycle delay was 3 s, giving 66−87 h per 3D experiment. The transfer efficiencies in 3D NCACO and NCOCA experiments were estimated from the comparison of the intensity of ^{13}C signal passed through the two mixing sequences with direct cross-polarization ^{13}C signal and were found to be 11−15%.

90 kHz CW and 86 kHz TPPM decoupling[25] was applied on the ^{1}H channel during mixing and evolution, respectively. The sampling of $t1$ and $t2$ dimensions was synchronized with sample rotation to eliminate the spinning sidebands. In $t1$ and $t2$, 96 and 52−68 points were collected, respectively, giving a t_1 max value of 10.7 ms and a t_2 max value of 5.8−7.6 ms. The TPPI method was used for phase-sensitive detection. The final spectral width in both indirect dimensions was 2250 Hz.

Data were processed using FELIX (Accelrys, San Diego, CA). Indirect ^{15}N and ^{13}C dimensions were zero-filled to 256 and 128 points, respectively. A Gaussian apodization function with a line-broadening parameter of 50 Hz was applied to the directly detected dimension, while cosine bell apodization functions were applied to both indirect dimensions. The carbon dimension was referenced externally to TMS, using the ^{13}C adamantane methylene peak at 38.56 ppm. The referencing was then readjusted to DSS assuming a 1.7 ppm chemical shift difference between TMS and DSS.[30] The nitrogen dimension was referenced externally to ammonium chloride (^{15}N chemical shift of 35.9 ppm relative to liquid ammonia at −50 °C) and readjusted to liquid ammonia at 25 °C by subtracting 3.37 ppm.[31] The spectra were assigned using Sparky.[32] A Gaussian fit of the histogram showing the distribution of chemical shift differences was carried out using Igor Pro (WaveMetrics, Oregon). Chemical shift index analysis was done using CSI (v. 2.0).[33]

Results

Pulse Sequences. The assignment strategy is conceptually very similar to that commonly used for solution NMR.[34−36] The backbone assignments reported herein were carried out exclusively at a moderate applied magnetic field strength. To compensate the moderate dispersion at 400 MHz, three 3D experiments were implemented: NCOCA, NCACO, and NCACX correlations. The polarization transfer pathways for these experiments are shown in Figure 3. The DCP sequence[23,37] was used to transfer polarization within the directly bonded ^{15}N−^{13}C pairs; this sequence operates by simultaneously applying the spin-lock radio frequency pulses to the corresponding radio frequency channels with the amplitudes of spin-locked fields adjusted such that the nutation frequencies of I and S spins satisfy the Hartmann−Hahn matching condition:[38] $\omega_{1I} = \omega_{1S} \pm n\omega_r$, where

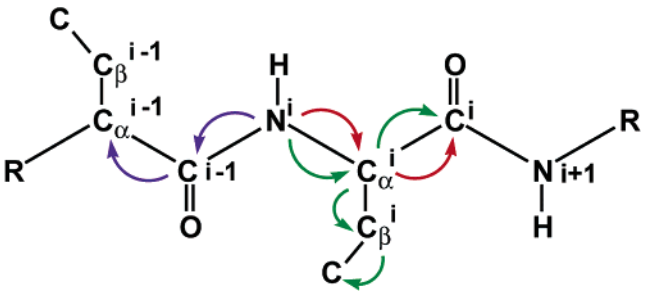

Figure 3. Polarization transfer pathways for NCOCA (blue), NCACO (red), and NCACX (green) experiments.

ω_r is the spinning frequency and n is an integer. An adiabatic transfer[39] with a linear amplitude modulation[22] was used to selectively transfer from the amidic nitrogen to either the carbonyl or the methine.[24] In model compounds, 40−60% transfer efficiencies for directly bonded spin pairs were reported.[24] In uniformly ^{13}C,^{15}N-enriched ubiquitin, 35−40% transfer efficiencies were achieved at 9.4 T. Spin diffusion or the so-called "^{13}C−^{1}H dipolar-assisted rotational resonance" experiment[28] and RFDR were used for homonuclear recoupling, principally for Cα−Cβ and Cα−CO recoupling, respectively. The polarization transfer pathways which we made use of in solid-state NMR experiments differ in that the ^{1}H nucleus was not used for detection; protons were used simply to enhance the polarization of ^{15}N via the initial cross-polarization step.

Backbone Correlations. In these correlation experiments, each nitrogen atom correlates to its own carbonyl and Cα in the NCACO experiment and to the preceding carbonyl and Cα in the NCOCA experiment. The NCACX experiment provides the correlations to the side-chain carbons, supplying information about the spin system type. Figure 4A,B shows two strip plots constructed from the 3D NCACO and NCOCA experiments. These plots, illustrating a backbone walk from Val17 to Asp32, provide an indication of the quality of the data and show regions with a varying degree of spectral resolution. The plots display amide nitrogen planes, with the Cα chemical shift and the CO chemical shifts as axes. The contour threshold was set at a value exceeding the RMS noise level of the spectra at least 8-fold, with the multiplier set to 1.2; the contour threshold levels for Pro19, Glu24, and Asn25/Glu24 cross-peaks are 43% lower than for the rest of the cross-peaks due to their lower intensity. Note that the "backbone walk" is interrupted between Asn25 and Val26 due to the absence of the Asn25 intraresidue correlation and the intraresidue NCαCO peak for Lys27 is not shown due to its coincidence with Leu56. The intraresidue cross-peak of Val26 is aliased in the Cα dimension and is shown to be connected to the K27/V26 cross-peak in the next NCOCA strip. In most cases, even when the "backbone walk" was interrupted due to unresolved or missing $N_iCO_{i-1}C\alpha_{i-1}$ correlations, the assignment of backbone carbons was still possible based on the intraresidue correlations involving backbone and side-chain carbon atoms. Strip plots for the rest of the backbone atoms are presented elsewhere.[40]

Amino Acid Side Chains from the NCACX Experiment. The homonuclear mixing time in the 3D NCACX experiment

(29) Boender, G. J.; Raap, J.; Prytulla, S.; Oschkinat, H.; de Groot, H. J. M. *Chem. Phys. Lett.* **1995**, *237*, 502−508.
(30) Wishart, D. S.; Bigam, C. G.; Yao, J.; Abildgaard, F.; Dyson, H. J.; Oldfield, E.; Markley, J. L.; Sykes, B. D. *J. Biomol. NMR* **1995**, *6*, 135−140.
(31) McDermott, A.; Gu, Z. In *Encyclopedia of Nuclear Magnetic Resonance*; Grant, D. M., Harris, R. K., Eds.; Wiley: New York, 1996; pp 1137−1147.
(32) Goddard, T. D.; Kneller, D. G. *SPARKY 3*; University of California: San Francisco, CA.
(33) Wishart, D. S.; Sykes, B. D. *J. Biomol. NMR* **1994**, *4*, 171−180.
(34) Bax, A.; Grzesiek, S. *Acc. Chem. Res.* **1993**, *26*, 131−138.
(35) Clore, G. M.; Gronenborn, A. M. In *Encyclopedia of Nuclear Magnetic Resonance*; Grant, D. M., Harris, R. K., Eds.; Wiley: New York, 1994; Vol. 7, pp 4744−4752.
(36) Clore, G. M.; Gronenborn, A. M. *Curr. Opin. Chem. Biol.* **1998**, *2*, 564−570.
(37) Stejskal, E. O.; Schaefer, J.; McKay, R. A. *J. Magn. Reson.* **1984**, *57*, 471−485.
(38) Stejskal, E. O.; Schaefer, J.; Waugh, J. S. *J. Magn. Reson.* **1977**, *28*, 105−112.
(39) Baldus, M.; Geurts, D. G.; Hediger, S.; Meier, B. H. *J. Magn. Reson., Ser. A* **1996**, *118*, 140−144.
(40) Igumenova, T. I. Ph.D. Thesis, Columbia University, New York, NY, 2003.

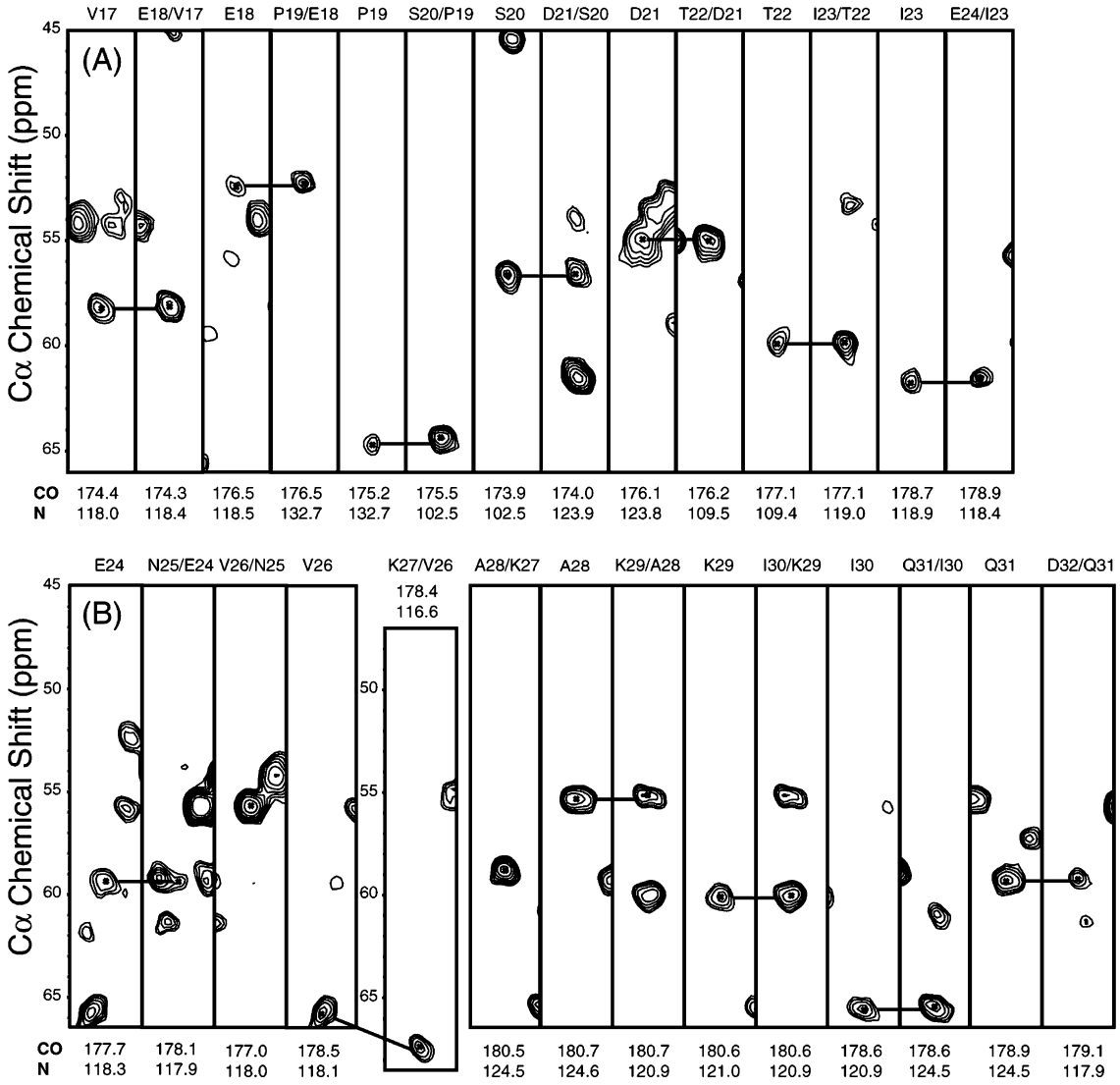

Figure 4. Val17-Asp32 strip plot constructed from the amide nitrogen planes of the NCOCA and NCACO experiments. The strips are 3.2 ppm wide in the carbonyl dimension. The solid lines connect cross-peaks that have the same Cα and CO chemical shifts but belong to different amide nitrogen planes.

(6.7 ms) was optimized to provide Cα−Cβ correlations, based on monitoring the intensity of the Cβ region in 1D protein spectra as a function of spin diffusion mixing time. However, a number of two-bond correlations were also observed and were very useful for confirming assignments. Several examples of ^{13}C protein side chain spectra are shown in Figure 5, illustrating the functional groups that typically showed clear diagnostic signals. The side-chain spectra of Thr22, Val26, Ile30, and Ile44 have pronounced Cα−Cγ cross-peaks, while the side chains of Lys33 and Met1 have only single-bond Cα−Cβ cross-peaks. Unambiguous Cα−Cβ correlations were observed for 50 amino acids out of a possible 70; ^{13}C spectra of these side chains are given elsewhere.[40] Two regions are missing form the data, the first loop and the C-terminus, thus reducing the number of Cα−Cβ correlations to 63. This issue will be elaborated further in the Discussion section.

Discussion

Selection of Pulse Sequences and Comparisons with Other Recent Work. To summarize, for all three experiments, we elected to use the DCP mixing sequence for ^{15}N−^{13}C polarization transfer. For CO−Cα recoupling, we chose RFDR; at spinning frequencies of 9−10 kHz, this sequence can be made selective toward CO−Cα recoupling. For the NCACX experiment, we implemented spin diffusion to obtain correlations between Cα and other side-chain carbons. Using this set of 3D experiments, we obtained sequential assignments for the majority of sites in ubiquitin. This approach may be contrasted with the assignment strategy used in other work to assign an SH3 domain. A variety of pulse sequences or methods have been used for homonuclear recoupling and recording homonuclear correlations in uniformly enriched materials; these range from simple methods such as spin diffusion[41] or RFDR,[27,42] to sophisticated adiabatic pulse sequences such as DREAM[43,44] or elegant rotor-synchronized methods such as C7 and its

(41) Szeverenyi, N. M.; Sullivan, M. J.; Maciel, G. E. *J. Magn. Reson.* **1982**, *47*, 462−475.
(42) Bennett, A. E.; Ok, J. H.; Griffin, R. G.; Vega, S. *J. Chem. Phys.* **1992**, *96*, 8624−8627.
(43) Verel, R.; Baldus, M.; Ernst, M.; Meier, B. H. *Chem. Phys. Lett.* **1998**, *287*, 421−428.
(44) Verel, R.; Ernst, M.; Meier, B. H. *J. Magn. Reson.* **2001**, *150*, 81−99.

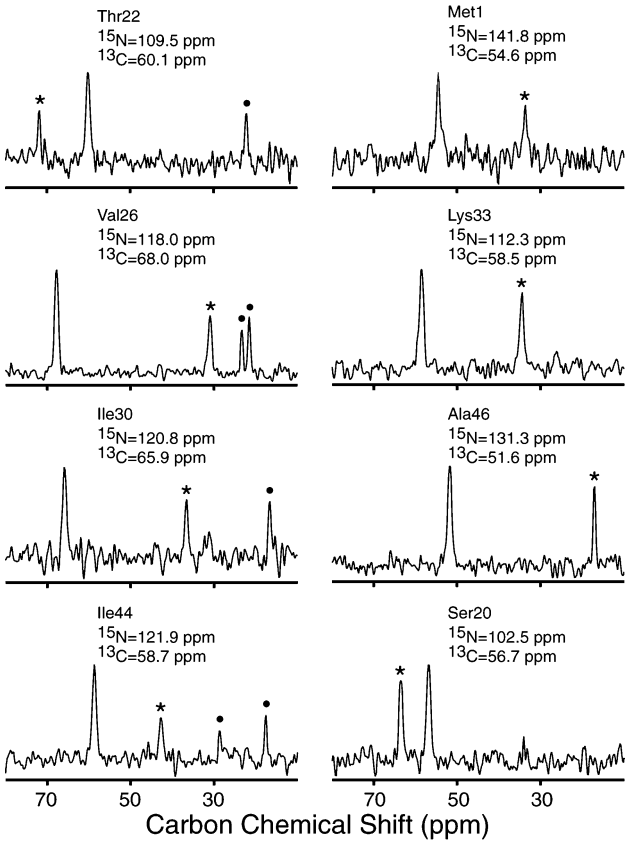

Figure 5. ^{13}C spectra of several protein side chains extracted from the 3D NCACX experiment. Resonances corresponding to Cβ and Cγ atoms are indicated with asterisks and dots, respectively. The left column shows examples of side chains for which two-bond C$\alpha-$Cγ correlations were observed.

variants.[45,46] An application of the band-selective DREAM sequence was recently reported for the SH3 domain of α-spectrin.[20] A set of complementary 2D $^{15}N/^{13}C$ experiments carried out at 17.6 T yielded almost complete ^{13}C and ^{15}N assignments.[20] Furthermore, our scheme made no use of proton chemical shifts, whereas 3D $^{1}H-^{13}C-^{13}C$ experiments resulted in the assignment of nonexchanging protons.[21] A recent solid-state NMR study showed that protons could be efficiently used as relays to obtain long-range $^{13}C-^{13}C$ correlations in ubiquitin,[47] but this method was not used here. Our work illustrates that heteronuclear higher dimensional experiments at moderate field strengths allow unambiguous assignments.

Verification and Completeness. The sequential assignments were verified, and additional carbon assignments of protein side chains were obtained in a 2D $^{13}C-^{13}C$ spin diffusion experiment carried out at a high applied magnetic field strength of 800 MHz and heteronuclear experiments at 600 MHz, both of which will be described in detail in forthcoming papers. In our 3D data sets, we were able to detect 62 out of possible 75 sequential connectivities (83%) and 50 C$\alpha-$Cβ side-chain resonances out of a possible 70 (71%). In combination with the high-field $^{13}C-^{13}C$ correlation experiments, 67 spin systems out of 76 total, or 88%, were assigned.

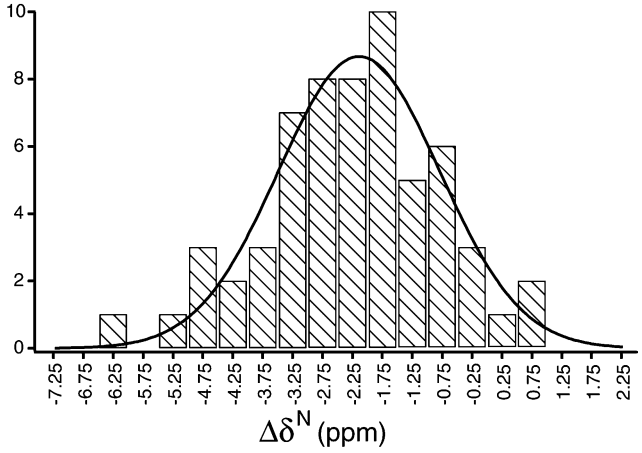

Figure 6. Histogram of the observed ^{15}N chemical shift differences between solid- and solution-state NMR. The chemical shift difference is defined as $\Delta\delta^N = \delta^N_{solid} - \delta^N_{solution}$. The solid line represents a fit of the histogram using a Gaussian function $y = A \exp\{-[(x - x0)/width]^2\}$. $x0$ and width best-fit parameters were found to be -2.163 ± 0.099 and 1.908 ± 0.140, respectively. The standard deviation of the mean σ is trivially calculated from the width parameter and is equal to 1.349 ± 0.099.

Table 1. Backbone Carbon and Nitrogen Chemical Shift Outliers[a]

N			Cα			CO		
residue	$\Delta\Delta\delta^N$ (ppm)[b]	2° structure[c]	residue	$\Delta\Delta\delta^{C\alpha}$ (ppm)	2° structure	residue	$\Delta\Delta\delta^{CO}$ (ppm)	2° structure
Thr7	2.7	S/T[d]	His68	−1.4	S	Leu71	−2.5	S
Glu24	−2.2	H	**Asp32**	−1.2	H	Lys63	−1.6	T
Asn25	−2.8	H	**Asn60**	−0.7	U	**Asn25**	−1.4	H
Val26	−3.3	H	Lys29	0.8	H	**Asn60**	−1.1	U
Lys33	−2.4	H	Phe45	2.8	S/T[d]	Ser20	−0.9	T
Leu50	2.5	U				**Asp32**	−0.8	H
Glu64	−4.2	T				**Glu64**	−0.8	T
Ser65	−2.6	T				Ile3	−0.7	S
Thr66	3.1	S				Gln41	0.7	S
						Gln62	0.7	T

[a] Residues, for which at least two *backbone* chemical shifts are perturbed, are shown in bold. [b] Chemical shift difference is calculated relative to the center of the Gaussian curve. [c] Secondary structure in 1UBQ as defined by PROMOTIF;[54] T is β-turn, H is α-helix, S is β-strand, and U is undefined. [d] Assigned to both elements of secondary structure by PROMOTIF.

There are two stretches of amino acids that are systematically missing from all available data sets; the first region includes residues Leu8-Lys11 and corresponds to the β-turn between the first two β-strands of ubiquitin. The second region includes five residues of ubiquitin C-terminus, Arg72-Gly76. The 13 missing C$\alpha-$Cβ peaks in our 3D NCACX spectrum include Gln2, Thr7, Glu24, Asn25, Arg42, Phe45, Glu51, Asp52, Tyr59, Gln62, Thr66, Leu67, and His68. Both missing regions show depressed values of generalized order parameters in solution NMR,[4] which is indicative of subnanosecond backbone motions (in agreement with other solution NMR studies of ubiquitin[48,49]). The C-terminus and Leu8-Gly10 region have crystallographic temperature factors that exceed the average value for all atoms and water molecules in ubiquitin.[7] We speculate that the residues from these regions are missing from the spectra because backbone motions cause poor performance

(45) Hohwy, M.; Jakobsen, H. J.; Eden, M.; Levitt, M. H.; Nielsen, N. C. *J. Chem. Phys.* **1998**, *108*, 2686−2694.
(46) Hohwy, M.; Rienstra, C. M.; Jaroniec, C. P.; Griffin, R. G. *J. Chem. Phys.* **1999**, *110*, 7983−7992.
(47) Lange, A.; Luca, S.; Baldus, M. *J. Am. Chem. Soc.* **2002**, *124*, 9704−9705.
(48) Lienin, S. F.; Bremi, T.; Brutscher, B.; Bruschweiler, R.; Ernst, R. R. *J. Am. Chem. Soc.* **1998**, *120*, 9870−9879.
(49) Fushman, D.; Tjandra, N.; Cowburn, D. *J. Am. Chem. Soc.* **1999**, *121*, 8577−8582.

Table 2. Comparison of Solid- and Solution-State ^{15}N NMR Chemical Shifts for Uniformly ^{13}C,^{15}N-Enriched Ubiquitin[a]

residue	δ^N_{solid}	$\delta^N_{solution}$ (pH 5.7)[b]	$\Delta\delta^N$ (pH 5.7)	$\delta^N_{solution}$ (pH 4.5)[c]	$\Delta\delta^N$ (pH 4.5)	residue	δ^N_{solid}	$\delta^N_{solution}$ (pH 5.7)[b]	$\Delta\delta^N$ (pH 5.7)	$\delta^N_{solution}$ (pH 4.5)[c]	$\Delta\delta^N$ (pH 4.5)
Gln2	124.3	124.5	−0.2	123.3	1.0	Asp39	112.2	115.1	−2.9	113.3	−1.1
Ile3	115.8	116.7	−0.9	115.3	0.5	Gln40	116.2	118.4	−2.2	116.8	−0.6
Phe4	117.6	120.1	−2.5	117.9	−0.3	Gln41	117.5	119.5	−2.0	117.7	−0.2
Val5	119.8	122.8	−3.0	120.8	−1.0	Arg42	120.2	124.5	−4.3	122.7	−2.5
Lys6	127.4	129.4	−2.0	127.4	0.0	Leu43	122.6	125.9	−3.3	123.9	−1.3
Thr7	*117.4*	*116.9*	*0.5*	*115.4*	*2.0*	Ile44	122.0	123.8	−1.8	121.9	0.1
Thr12	119.5	122.1	−2.6	120.4	−0.9	Phe45	124.4	126.6	−2.2	125.3	−0.9
Ile13	127.0	129.1	−2.1	126.9	0.1	Ala46	131.4	134.2	−2.8	132.3	−0.9
Thr14	121.2	123.2	−2.0	121.4	−0.2	Gly47	102.2	104.0	−1.8	102.3	−0.1
Leu15	123.9	126.7	−2.8	124.6	−0.7	Lys48	119.5	123.5	−4.0	121.5	−2.0
Glu16	122.0	124.0	−2.0	122.0	0.0	Gln49	121.4	124.5	−3.1	122.3	−0.9
Val17	118.0	119.0	−1.0	117.1	0.9	*Leu50*	*127.5*	*127.2*	*0.3*	*125.4*	*2.1*
Glu18	118.4	120.9	−2.5	118.7	−0.3	Glu51	123.3	124.6	−1.3	122.8	0.5
Ser20	102.5	105.0	−2.5	103.2	−0.7	Asp52	120.3	121.8	−1.5	120.0	0.3
Asp21	123.9	125.4	−1.5	123.4	0.5	Arg54	118.1	120.8	−2.7	119.1	−1.0
Thr22	109.4	110.5	−1.1	108.8	0.6	Thr55	108.6	110.4	−1.8	108.2	0.4
Ile23	118.9	122.7	−3.8	121.2	−2.3	Leu56	117.2	119.6	−2.4	117.8	−0.6
Glu24	*118.3*	*122.7*	*−4.4*	*120.7*	*−2.4*	Ser57	112.3	115.0	−2.7	113.2	−0.9
Asn25	*117.9*	*122.9*	*−5.0*	*120.3*	*−2.4*	Asp58	124.4	126.0	−1.6	124.1	0.3
Val26	*118.1*	*123.6*	*−5.5*	*121.6*	*−3.5*	Tyr59	114.6	117.3	−2.7	115.5	−0.9
Lys27	116.4	120.4	−4.0	118.9	−2.5	Asn60	117.4	117.5	−0.1	115.9	1.5
Ala28	124.5	124.9	−0.4	123.4	1.1	Ile61	117.0	120.4	−3.4	118.5	−1.5
Lys29	121.0	121.7	−0.7	119.9	1.1	Lys63	119.0	122.1	−3.1	120.2	−1.2
Ile30	120.9	122.8	−1.9	121.1	−0.2	*Glu64*	*109.7*	*116.1*	*−6.4*	*113.7*	*−4.0*
Gln31	124.5	125.1	−0.6	123.4	1.1	*Ser65*	*111.6*	*116.4*	*−4.8*	*114.7*	*−3.1*
Asp32	117.7	121.2	−3.5	119.3	−1.6	*Thr66*	*119.8*	*118.9*	*0.9*	*117.0*	*2.8*
Lys33	*112.3*	*116.9*	*−4.6*	*115.0*	*−2.7*	His68	117.5	120.9	−3.4	118.2	−0.7
Glu34	112.4	115.9	−3.5	113.5	−1.1	Leu69	124.6	125.5	−0.9	124.4	0.2
Gly35	109.4	110.4	−1.0	108.6	0.8	Val70	126.4	128.2	−1.8	127.2	−0.8
Ile36	119.4	121.7	−2.3	119.9	−0.5	Leu71	123.2	124.6	−1.4	123.2	0.0

[a] Residues with perturbed chemical shifts in the solid state (relative to solution) are italicized. [b] Wand, A. J.; Urbauer, J. L.; McEvoy, R. P.; Bieber, R. J. *Biochemistry* **1996**, *35*, 6116−6125. [c] Courtesy of Professor David Fushman, University of Maryland.

in the polarization transfer sequences. The poor transfer efficiencies may result from intermediate exchange effects, or alternatively, they may result from low order parameters and high asymmetry parameters for the time-averaged dipolar couplings. An alternative explanation for the missing cross-peaks is the conformational heterogeneity of certain protein regions that could produce severe inhomogeneous broadening of the resonances. However, the solution NMR data strongly support the dynamics view.

Comparison of Solution- and Solid-State Chemical Shifts of Ubiquitin. Previously, several groups attempted to establish whether there is a general agreement between solution- and solid-state NMR chemical shifts in proteins. Remarkable agreement was found for ^{15}N chemical shifts of staphylococcal nuclease, and the solution chemical shifts were used to provide site-specific assignment for the solid state.[14] In the case of the cyclic decapeptide antanamide, Meier's group compared ^{13}C chemical shifts for different preparations of solid and solution samples and found chemical shift variations of up to 2.8 ppm.[50] For the first protein assigned in the solid-state, 62-residue SH3 domain of α-spectrin,[20] solid-state ^{13}C NMR chemicals shifts were demonstrated to be suitable for secondary chemical shift analysis.[51] While the experimental evidence is still very limited, there seems to be a *general* agreement between protein chemical shifts observed in solution and the solid state, a logical result of the fact that the structures are generally similar.

To carry out a comparison between solid-state and solution ^{15}N chemical shifts of ubiquitin, we chose a set of ^{15}N solution chemical shifts reported by Wand et al.[3] It is expected that some of the residues should be shifted and that the shifts are informative about structural issues. Despite the fact that the structure of ubiquitin is very similar in solution and solid state, the solvent and the ionization state of the protein is probably different, which could have an important effect on the chemical shifts. Solution NMR studies were carried out at pH 5.7 in phosphate buffer, while the solid-state NMR sample was at pH 4.0−4.2 in citrate buffer. Also, a typical crystalline protein has many of its exposed residues in intermolecular contacts, and a precipitated or microcrystalline protein probably does as well. We expect to see perturbation in the chemical shifts of those residues involved in packing contacts, typically a fraction of the surface-exposed residues.

To account for the difference in the referencing procedures, we constructed a histogram of chemical shift differences, defined as $\Delta\delta^N = \delta^N_{solid} - \delta^N_{solution}$. The bin size was chosen to be 0.5 ppm, which exceeds the average standard deviation of all ^{15}N resonances within solid-state NMR data, 0.08 ppm, more than 5-fold. (Thus, the probability that a given chemical shift falls into the correct bin is greater than 95%.) The histogram contains 60 observations and is shown in Figure 6. The histogram was then fit using a Gaussian curve, with a maximum at −2.163 ppm and a width of 1.908 ppm (see the caption of Figure 6). We define the outliers as protein residues for which ^{15}N chemical shift differences fall outside an 89% confidence interval, i.e., outside the interval of $\pm 1.6\sigma$ relative to the center of the Gaussian curve. A full list of solid- and solution-state

(50) Detken, A.; Hardy, E. H.; Ernst, M.; Kainosho, M.; Kawakami, T.; Aimoto, S.; Meier, B. H. *J. Biomol. NMR* **2001**, *20*, 203−221.

(51) Luca, S.; Filippov, D. V.; van Boom, J. H.; Oschkinat, H.; de Groot, H. J. M.; Baldus, M. *J. Biomol. NMR* **2001**, *20*, 325−331.

^{15}N NMR chemical shifts of ubiquitin are given in Table 2 and elsewhere.[40] Table 1 shows amino acid outliers, with chemical shift differences calculated relative to the position of the Gaussian curve maximum, along with information about the secondary structure.

To compare the Cα and CO chemical shifts of ubiquitin in solution and solid state, we used the same procedure as for the ^{15}N chemical shifts. For the analysis of Cα chemical shifts, we selected 63 residues for which secure assignments in both solid and solution state were available. For the CO analysis, a similar subset of residues was chosen. The average standard deviation of ^{13}C chemical shifts, taken over all cross-peaks with assignment count larger than two, is 0.11 ppm. Thus, the bin size is approximately 5 times the standard deviation of the mean carbon chemical shift, which ensures >95% probability that a given value of chemical shift falls into the bin. A full list of solid- and solution-state ^{13}C NMR chemical shifts is given in Table 3 and elsewhere,[40] while the outliers are listed in Table 1.

The histograms for Cα and CO chemical shift differences are presented in Figure 7. Note that the systematic shift of the histogram maxima observed for all three groups of atoms (N, CO, and Cα) is due to different referencing procedures used in solution- and solid-state NMR. The width of the chemical shift difference distribution, characterized by the standard deviation of the mean σ, was almost identical for CO and Cα and was found to be ~0.4 ppm. In contrast, the width of the distribution for ^{15}N shifts was more than 3 times higher: 1.3 ppm. Residues with more than one chemical shift (among Cα, Cβ, CO, and N) strongly perturbed include: Asn25, Asp32, Gln41, Leu50, Asn60, Gln62, Glu64, and Ser65. Since there is yet no reported full structure for ubiquitin under conditions similar to those of our solid-state NMR experiments, we cannot establish whether crystal-packing forces are responsible for the observed perturbation of chemical shifts. Although most amino acids with perturbed chemical shifts are polar, there is no clear correlation with accessible surface area.

In Figure 8, the amino acids for which at least two solid-state NMR chemical shifts deviate significantly from the corresponding solution values are mapped onto the X-ray structure of ubiquitin (1UBQ)[7] and shown in ball-and-stick representation. Asn25 and Asp32 are located on the solvent-exposed part of the ubiquitin α helix. Gln41 forms the beginning of the β-strand, with its side chain packed against the α helix. Leu50 does not have any secondary structure assigned to it and occurs at the beginning of the β-turn region comprising residues 51−54. In the primary sequence, two polar residues on each side surround Leu50: -K48-Q49-L50-E51-D52-. Asn60 is located at the end of the 3/10 helix and precedes the Gln62-Ser65 β-turn. Gln62, Glu64, and Ser65 belong to the same β-turn, which is highly solvent-exposed.

The backbone conformation of ubiquitin is constant over a wide pH range.[52] On the other hand, pH appears to be an important factor in modulating ubiquitin-mediated signaling; in a recent solution NMR study, the ubiquitin dimer switches its conformation from open to closed state with increasing pH.[53] We considered the possibility that the pH-related changes in the local charge distributions were responsible for the differences between the shifts measured at pH 6.5 in solution vs pH 4.0−4.2 in the solid state. A comparison between our reported shifts and the chemical shifts from a solution NMR study at pH 4.5 still identifies the same sites as outliers. Thus, we speculate that

Table 3. Comparison of Solid- and Solution-State ^{13}CO and ^{13}Cα NMR Chemical Shifts for Uniformly ^{13}C,^{15}N-Enriched Ubiquitin[a]

residue	δ^{CO}_{solid}	$\delta^{CO}_{solution}$ [b]	$\Delta\delta^{CO}$	residue	$\delta^{C\alpha}_{solid}$	$\delta^{C\alpha}_{solution}$	$\Delta\delta^{C\alpha}$
Met1	170.7	171.4	−0.7	Met1	54.4	54.7	−0.3
Gln2	176.4	176.9	−0.5	Gln2	54.8	55.4	−0.6
Ile3	*171.7*	*173.2*	*−1.5*	Ile3	59.3	59.9	−0.6
Phe4	175.4	176.0	−0.6	Phe4	54.1	55.3	−1.2
Val5	174.5	175.7	−1.2	Val5	60.4	60.7	−0.3
Lys6	177.6	178.0	−0.4	Lys6	54.2	54.8	−0.6
Thr7	176.7	177.8	−1.1	Thr7	60.3	60.7	−0.5
Thr12	174.1	175.2	−1.1	Thr12	61.5	62.6	−1.1
Ile13	175.5	176.1	−0.6	Ile13	59.9	60.3	−0.4
Thr14	173.9	174.6	−0.7	Thr14	61.8	62.3	−0.5
Leu15	174.7	175.4	−0.7	Leu15	52.9	53.0	−0.1
Glu16	175.9	176.7	−0.8	Glu16	54.6	55.2	−0.6
Val17	174.3	174.9	−0.6	Val17	58.2	58.8	−0.6
Pro19	175.2	176.2	−1.0	Glu18	52.4	53.0	−0.6
Ser20	*173.8*	*175.5*	*−1.7*	Pro19	64.8	65.6	−0.8
Asp21	176.1	177.2	−1.1	Ser20	56.8	57.7	−0.9
Thr22	177.0	177.6	−0.6	Asp21	55.1	56.1	−1.0
Ile23	178.7	179.8	−1.1	Thr22	60.0	60.0	0.0
Asn25	*177.0*	*179.2*	*−2.2*	Ile23	61.7	62.7	−1.0
Val26	178.3	178.8	−0.5	Asn25	55.9	56.3	−0.4
Lys27	180.4	181.4	−1.0	Val26	67.8	67.9	−0.1
Ala28	180.6	181.1	−0.5	Lys27	59.1	59.5	−0.4
Lys29	180.5	181.1	−0.6	Ala28	55.4	55.6	−0.2
Ile30	178.5	179.1	−0.6	*Lys29*	*60.3*	*60.1*	*0.2*
Gln31	178.8	179.7	−0.9	Ile30	65.8	66.4	−0.7
Asp32	*176.6*	*178.2*	*−1.6*	Gln31	59.4	60.4	−1.0
Lys33	178.0	178.7	−0.7	*Asp32*	*55.9*	*57.7*	*−1.8*
Glu34	178.0	178.8	−0.8	Lys33	58.5	58.5	0.0
Gly35	173.5	174.8	−1.3	Glu34	55.1	55.6	−0.5
Pro38	178.3	179.1	−0.8	Gly35	45.4	46.2	−0.8
Asp39	176.9	177.9	−1.0	Ile36	57.4	58.0	−0.6
Gln40	175.0	176.3	−1.3	Pro37	61.5	61.8	−0.3
Gln41	*176.9*	*177.0*	*−0.1*	Pro38	66.0	66.5	−0.5
Arg42	174.5	174.7	−0.2	Asp39	55.2	56.0	−0.8
Leu43	175.5	176.2	−0.7	Gln40	55.3	55.8	−0.5
Ile44	176.3	176.7	−0.4	Gln41	55.9	56.9	−1.0
Phe45	174.4	175.5	−1.1	Arg42	54.5	55.4	−0.9
Ala46	177.9	178.2	−0.3	Leu43	52.5	53.3	−0.8
Gly47	173.7	174.6	−0.9	Ile44	58.7	59.2	−0.5
Lys48	175.0	175.5	−0.5	*Phe45*	*59.1*	*56.8*	*2.3*
Gln49	176.1	176.4	−0.3	Ala46	51.8	52.8	−1.0
Leu50	176.9	177.5	−0.6	Gly47	45.5	45.5	0.0
Glu51	175.6	176.3	−0.7	Lys48	53.9	54.8	−0.9
Gly53	174.4	175.6	−1.2	Gln49	55.8	56.2	−0.4
Arg54	175.5	176.2	−0.7	Leu50	54.3	54.5	−0.2
Thr55	176.6	177.4	−0.8	Glu51	55.5	56.1	−0.6
Leu56	180.5	181.6	−1.1	Gly53	44.6	45.4	−0.8
Ser57	178.4	179.1	−0.7	Arg54	53.9	54.5	−0.6
Asp58	177.7	178.3	−0.6	Thr55	59.4	60.0	−0.6
Tyr59	174.6	175.5	−0.9	Leu56	58.6	58.9	−0.3
Asn60	*173.2*	*175.1*	*−1.9*	Ser57	61.2	61.4	−0.2
Ile61	175.1	175.4	−0.3	Asp58	57.3	57.7	−0.4
Gln62	*176.6*	*176.7*	*−0.1*	Tyr59	58.6	58.6	0.0
Lys63	*174.2*	*176.6*	*−2.4*	*Asn60*	*53.0*	*54.3*	*−1.3*
Glu64	*174.5*	*176.1*	*−1.6*	Ile61	61.8	62.7	−0.9
Ser65	171.7	172.9	−1.2	Gln62	53.5	53.9	−0.4
His68	173.7	174.6	−0.9	Lys63	57.2	58.2	−1.0
Leu69	175.2	176.2	−1.0	Glu64	58.0	58.7	−0.7
Val70	174.3	174.9	−0.6	Ser65	60.0	61.2	−1.2
Leu71	*175.4*	*178.7*	*−3.3*	*His68*	*54.3*	*56.3*	*−2.0*
				Leu69	53.9	54.0	−0.1
				Val70	60.2	60.9	−0.7
				Leu71	53.8	54.2	−0.4

[a] Residues with perturbed chemical shifts in the solid state (relative to solution) are italicized. [b] Wand, A. J.; Urbauer, J. L.; McEvoy, R. P.; Bieber, R. J. *Biochemistry* **1996**, *35*, 6116−6125.

(52) Ottiger, M.; Bax, A. *J. Biomol. NMR* **1999**, *13*, 187−191.
(53) Varadan, R.; Walker, O.; Pickart, C.; Fushman, D. *J. Mol. Biol.* **2002**, *324*, 637−647.

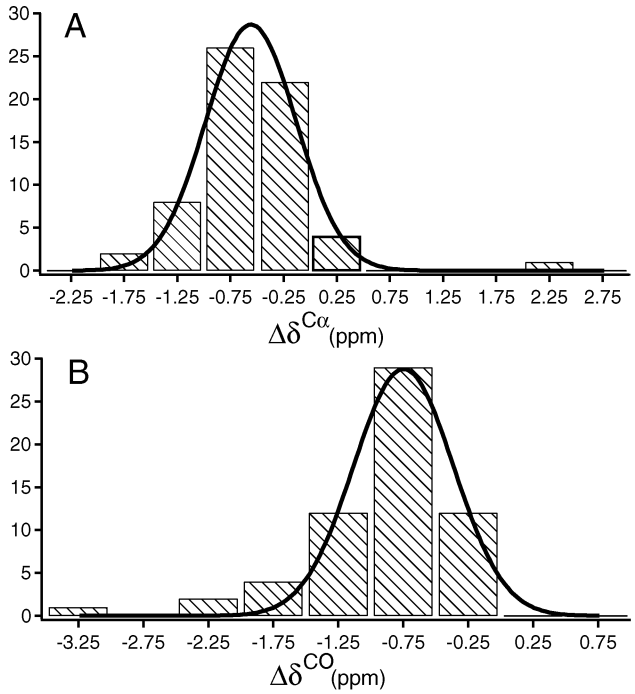

Figure 7. Histogram of the observed Cα (A) and CO (B) chemical shift differences between solid- and solution-state NMR. Gaussian fit of the histograms produced the following best-fit parameters: $x0 = -0.569 \pm 0.011$, width $= 0.603 \pm 0.016$, and $\sigma = 0.426 \pm 0.012$ for Cα; $x0 = -0.758 \pm 0.027$, width $= 0.544 \pm 0.032$, and $\sigma = 0.385 \pm 0.023$ for CO.

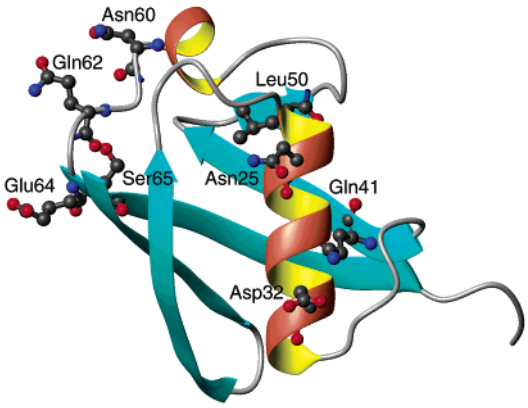

Figure 8. Ubiquitin residues with at least two chemical shifts of Co, Cα, Cβ, and N perturbed (ball-and-stick representation), mapped onto the crystal structure of ubiquitin.

contacts in the solid state may be responsible for the shifts reported here. It is also worth noting that, despite these perturbations, application of chemical shift index (CSI) methods[33] resulted in correct prediction of some secondary structure elements in ubiquitin. Figure 9 shows a plot of the consensus CSI obtained on the basis of Cα, Cβ, and CO chemical shifts. An index value of +1 indicates backbone torsion angles in the α-helical region, while an index value of −1 is consistent with the presence of the β-strand structures. For comparison, the results of the PROMOTIF analysis[54] for the ubiquitin crystal structure are plotted as a cartoon above the top axis of the graph. Most of the secondary structure elements are identified correctly, suggesting that solid-state NMR chemical shifts of proteins can be used for the CSI analysis.

Extending This Assignment Prospective for Membrane Proteins. One motivation for studying small soluble proteins in the solid state is the development of solid-state NMR methodology that would ultimately be applicable to intrinsic membrane proteins and other insoluble proteins. In that context, it is worth noting that partial (∼17%) assignments were recently reported for light harvesting complex II (94 residues, 10.1 kDa) at 17.6 T.[55] The assignment of at least three other membrane proteins is currently in progress: bacteriorhodopsin,[56] *c* subunit of ATP synthase, and light harvesting complex I (unpublished data). Some of the most important issues that are specific to membrane proteins involve sample handling. While preparation protocols involving batch crystallization work well for small soluble proteins, the crystallization of membrane proteins seems to be neither feasible nor practical for preparation of NMR samples, despite the fact that high-quality crystals are not required for solid-state NMR experiments. A viable alternative is the preparation of membrane protein samples by well-controlled precipitation in the presence of a detergent or membrane mimetic, which in our hands results in comparably narrow line widths. Another alternative would be the preparation of 2D membrane protein crystals, using procedures developed for cryoelectron microscopy.[57,58] From the ubiquitin study at moderate magnetic field strengths, we learned that line-narrowing protocols and additional digitization in the indirect dimension are not sufficient to carry out the resonance assignments using 2D spectroscopy: extension to one more chemical shift dimension was necessary to obtain a near-complete assignment of the protein backbone atoms. It is likely that for complete assignment of larger and less dispersed proteins such as intrinsic membrane

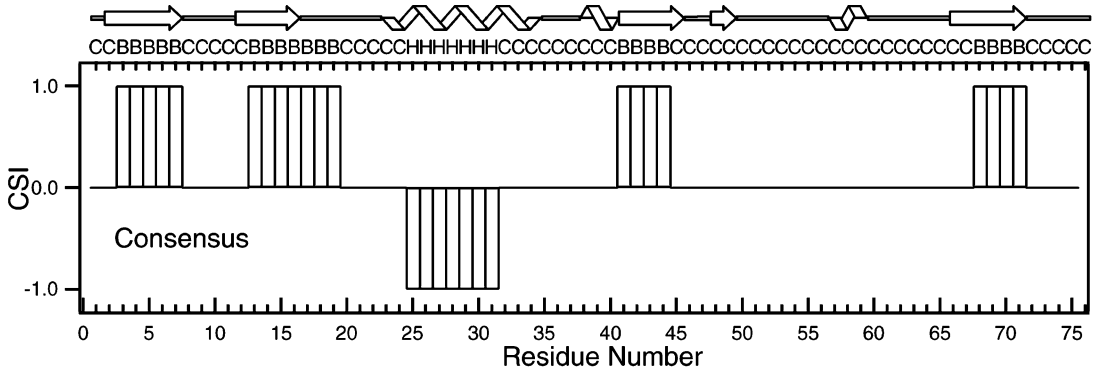

Figure 9. Consensus chemical shift index (CSI) analysis[33] of the ^{13}C solid-state NMR chemical shifts of ubiquitin. The consensus analysis was based on Cα, Cβ, and CO chemical shifts. The top X axis is labeled according to the following notation: "C" indicates coil, "B" indicates β-strand, and "H" indicates helix. For comparison, the secondary structure elements based on the PROMOTIF[54] analysis of the ubiquitin crystal structure are shown in the same figure.

systems, a combination of methods may be needed, e.g., isotope labeling schemes, J-decoupling, spectral editing techniques,[59] and possibly an extension to a fourth chemical shift dimension.

Summary

Ubiquitin is one of very few proteins assigned to this degree of completeness using solid-state NMR methods. The simple method used here is likely to have applications in many more challenging systems. The sample preparation protocol developed in this work that results in solid-state NMR spectra with excellent resolution and the availability of resonance assignments for the majority of protein sites open up many exciting possibilities for further structural and dynamical characterization of ubiquitin using solid-state NMR methods.

Acknowledgment. We thank Professor David Fushman (University of Maryland) for making the ^{15}N chemical shifts of ubiquitin at pH 4.5 available to us. We thank Chad Rienstra for assistance in the installation of the spectrometer. A.E.M. and T.I.I. were supported by a grant from the National Science Foundation (MCB 9983581). A.J.W. was supported by NIH Grant DK39806.

JA030546W

(54) Hutchinson, E. G.; Thornton, J. M. *Protein Sci.* **1996**, *5*, 212−220.
(55) Egorova-Zachernyuk, T. A.; Hollander, J.; Fraser, N.; Gast, P.; Hoff, A. J.; Cogdell, R.; de Groot, H. J. M.; Baldus, M. *J. Biomol. NMR* **2001**, *19*, 243−253.
(56) McMahon, M. T.; Bizounok, M.; Herzfeld, J.; Griffin, R. G. Presented at the 43rd Experimental Nuclear Magnetic Resonance Conference, Orlando, FL, 2002.
(57) Kuhlbrandt, W. *Q. Rev. Biophys.* **1992**, *25*, 1−49.
(58) Hasler, L.; Heymann, J. B.; Engel, A.; Kistler, J.; Walz, T. *J. Struct. Biol.* **1998**, *121*, 162−171.
(59) Astrof, N. S.; Griffin, R. G. *J. Magn. Reson.* **2002**, *158*, 157−163.